The International Journal of Advanced Manufacturing Technology (2018) 99:1369–1378
https://doi.org/10.1007/s00170-018-2591-8

ORIGINAL ARTICLE

An analysis of the tool electrode working mechanism of grinding-aided electrochemical discharge machining of MMCs

Jiangwen Liu[1] · Zhibiao Lin[1] · Taiman Yue[2] · Zhongning Guo[1] · Shuzhen Jiang[1]

Received: 10 April 2018 / Accepted: 14 August 2018 / Published online: 22 August 2018

Abstract
The working mechanism of the tool electrode in grinding-aided electrochemical discharge machining (G-ECDM) of metal matrix composites process has been studied in this paper. A series of experiments have been conducted to study tool electrode clogging and damage under different processing conditions. Moreover, the grit volume fractions and average grit height of the G-ECDM tool electrode have been studied to discover the working mechanism of the tool. The experimental results have shown that in the G-ECDM situation, though it is possible for the grinding effect to cause tool clogging, the clogged materials may be removed by the polarity spark effect and thus a stable processing condition can be obtained. Moreover, the tool life of G-ECDM is much longer than that of ECDM. The reason for this phenomenon could be that the binding materials between the diamond grits of the tool surface are potentially protected by the clogged materials during the process.

Keywords G-ECDM · Metal matrix composites · Tool electrode

1 Introduction

Metal matrix composites (MMCs), as a combination of two or more constituents in which a relatively soft and ductile metal phase acts as "matrix" and a hard and brittle dispersive materials acts as reinforcement phase [1], have been widely used in modern engineering and industries, including but not limited to aerospace, electronics, automobile industries, and medical applications [2–5]. This is primarily due to their high specific strength and stiffness, good elevated temperature properties, and excellent wear resistance [6–9]. Indeed, both the physical and mechanical properties of MMCs are in many respects superior to those of their monolithic counterparts. However, the unique properties that make them appealing to use may prove to be hurdles to shaping these materials effectively. Thus, the successful implementation of these advanced materials is still largely dependent on how cost-effectively the component can be fabricated and transformed to the required final shape. It is accepted that MMCs are in general much more difficult to machine than their monolithic counterparts, whether or not conventional or unconventional techniques are used [10, 11]. This causes no surprise, since most of the reinforcement phases are hard ceramic materials and are harder compared to most commonly used carbide and high-speed steel (HSS) tools, and because of this, cubic boron nitride (CBN), chemical vapor deposition (CVD), and polycrystalline diamond (PCD) tools are often required [8, 12]. Apart from the extreme hardness of most of the reinforcement phases, the vast differences in physical, chemical, and mechanical properties between the metal matrix and the reinforcement phase have positioned MMCs as a group of notoriously difficult-to-machine materials.

In the field of conventional machining, though the amount of research studying the grinding of MMCs is much less than for turning, drilling and milling, etc., its research value is of significance because normally a good surface finish with less damage can be obtained using grinding [10, 13–15]. Unconventional machining techniques, such as laser [11, 16] and water jet [17, 18] machining, can achieve a fairly high material removal rate but would often be accompanied by some serious surface and subsurface defects which in many

✉ Shuzhen Jiang
piercejiang88@gmail.com

[1] School of Electromechanical Engineering, Guangdong University of Technology, No.100 Waihuanxi Road, Guangzhou Higher Education Mega Center, Panyu District, Guangzhou 510006, People's Republic of China

[2] The Advanced Manufacturing Technology Research Centre, Department of Industrial and Systems Engineering, The Hong Kong Polytechnic University, Hung Hom, Hong Kong

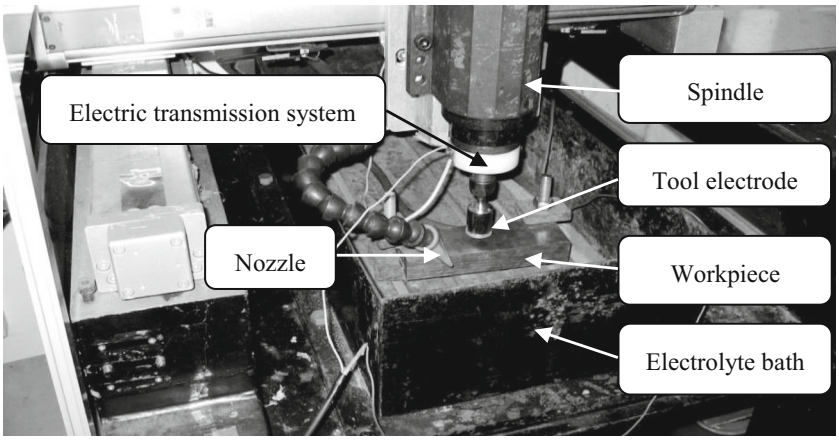

Fig. 1 Photo of the experimental equipment

cases are unacceptable to the final finished product and could undermine the fatigue strength of the final product. Moreover, these two machining methods are not ideally suited to 3-D shaping purposes. Among the many unconventional machining methods, electrical discharge machining (EDM) [19–21], wire-EDM [22–24], and electrochemical machining (ECM) [25, 26] as well as their hybrid forms like electrochemical discharge machining (ECDM) [27], ultrasonic vibration EDM (UEDM) [28], and powder mixed EDM (PEDM) [29, 30] are perhaps the most promising processes for shaping MMCs when the quality of surface finish and flexibility of shaping geometry are considered. Notwithstanding the merits of these two kinds of machining methods, there are still problems which need to be solved and improvements to be made before they can be effectively utilized for shaping MMCs.

The main problems encountered in EDM of MMCs are low machining rate [19, 31], high risk of tool breakage [23], entrapment of debris in the gap [32], and the presence of various forms of defects at the machined surface [19, 33]. On the other hand, close dimensional control is one of the most important issues that needed to be addressed in ECM [34]. These are mainly caused by the non-conducting nature of the ceramic reinforcement phase and often the segregation of the ceramic phase. The problems intensify as the extent of the ceramic phase increases. When employing the electrochemical discharge machining method, though the material removal rate can be much higher than that of EDM and ECM, the machined surface quality still needs to be improved and the tool electrode wear problem also needs to be solved [35].

Based on the above discussion, the authors propose a novel hybrid process combining the advantages of the grinding effect and the ECDM effect, namely the grinding-aided electrochemical discharge machining (G-

Table 1 Major specifications of the experiment equipment

	X-axis	*Y*-axis	*Z*-axis	Spindle	Electrical source	Electrolyte bath
Travel (mm)	250	250	100			
Repeatability position accuracy (μm)	5	5	1			
Position accuracy (μm)	15	15	2			
Speed (rpm)				0–20,000		
Gripping range (mm)				Ø 0.5–10		
Power (kW)				1.5		
Peak current (A)					0.5–100	
Voltage (V)					20–120	
Pulse duration (μs)					4–400	
Duty cycle					1:1–1:10	
Maximum liquid level (mm)						200
Medium						Deionized water
						Electrolyte
Circulator flow (L/min)						0–20

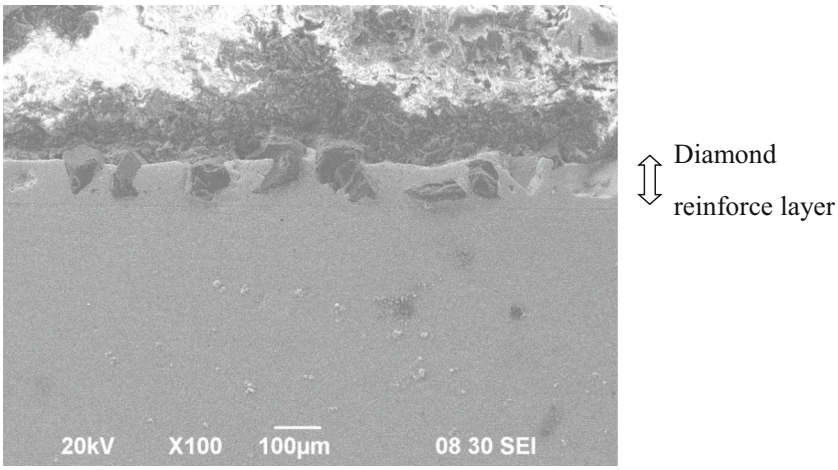

Fig. 2 SEM image of the diamond-reinforced layer of the tool electrode

ECDM) process to machine MMCs [36]. It was found that during the process, not only can a high material removal rate and good surface quality be obtained but also a low tool electrode wear rate can be achieved.

In order to discover the tool electrode working mechanism, this paper focuses on studying the tool performance of G-ECDM process. Other aspects of the study, such as the detailed material removal mechanism and spark generation mechanism, will be presented in a separate paper.

2 Materials and methods

Figure 1 shows the actual in-house built experimental equipment. Some major specifications of the experimental equipment are given in Table 1. To facilitate the study of the G-ECDM process, the experimental setup allows the number of electrical pulses to be preset.

The MMCs employed in this study was a particulate-reinforced aluminum 6061 with 10 vol% Al_2O_3 (10ALO). The material was in the form of rolled plates with the reinforcement particles having a nominal size of 21 μm. According to the working principle of the G-ECDM process, an appropriate steel drill tool with its surface reinforced with diamond grits of nominal size 120 μm has been designed. The diameter of the composite drill tool is 26 mm; the surface diamond-reinforced layer is about 100 μm thick (Fig. 2).

A 2.5 wt% $NaNO_3$ electrolyte was used for the G-ECDM and ECDM experiments, while deionized water was used for the EDM experiment. Other processing parameters can be found in Table 2.

During the course of G-ECDM of MMCs, if the grinding debris cannot be removed in time, some could adhere to the cathode-tool surface and when the trapped debris or chips between the diamond grits have increased to a certain amount, short-circuiting occurs. A schematic drawing showing grinding debris trapped in the tool is presented in Fig. 3. It is believed that EDM sparks could remove the clogged material that is trapped on the tool surface, and if the clogging materials can be removed by the EDM effect in time, stable machining conditions can be maintained. With this in mind, a computerized control system has been designed in this study. At the start of the process, the tool and the workpiece will be adjusted to a suitable processing position. Then, the tool will be fed with an initial set speed. If no unstable condition is encountered, the feed speed can be progressively increased to increase the grinding effect. Obviously, the amount of the

Table 2 Processing conditions for the study of tool surface condition

Processing conditions	A	B	C	D	E	F	G	H
Processing mode	Grinding	G-ECDM	G-ECDM	G-ECDM	ECDM	ECDM	ECDM	EDM
Peak current (A)	–	35	35	35	35	35	35	35
Applied voltage (V)	–	80	80	80	80	80	80	80
Pulse duration (μs)	–	48	48	200	48	48	48	48
Media	2.5% $NaNO_3$	2.5% $NaNO_3$	2.5% $NaNO_3$	2.5% $NaNO_3$	2.5% $NaNO_3$	2.5% $NaNO_3$	2.5% $NaNO_3$	Deionized water
Duty cycle	–	1:7	1:7	1:7	1:7	1:7	–	–
Spindle speed (rpm)	1500	1500	1500	1500	0	0	0	0
Processing time (min)	1	30	60	30	3	5	–	–

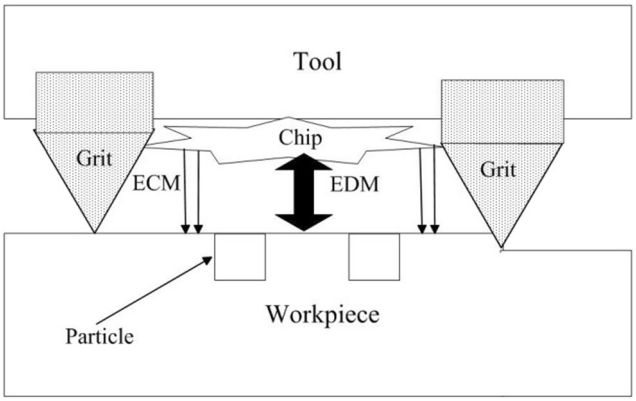

Fig. 3 Schematic diagram of machining debris trapped between diamond grits

clogging materials between the diamond grits increases correspondingly with an increase in the grinding effect. Though the increased amount of the clogging materials can facilitate the protection of the tool electrode from damage by the EDM effect, once these clogging materials which cannot be removed by the EDM effect in time have increased to a certain amount, short-circuiting would occur. Short-circuiting conditions are detected by monitoring a sudden drop of the processing voltage. When a short-circuiting is encountered, the tool will retract instantly and the feed speed will be reduced automatically to weaken the grinding effect. With this computerized control system, a balance between the clogging materials protection effect and EDM cleaning effect can be reached.

3 Results and discussion

3.1 A study of the clogging and damage of the G-ECDM tool electrode

Figure 4a–c shows the surfaces of the tools after direct grinding without the ECDM action (Table 2 condition A), G-ECDM for 30 min (Table 2 condition B), and G-ECDM for 60 min (Table 2 condition C), respectively. This section may be divided by subheadings. It should provide a concise and precise description of the experimental results and their interpretation as well as the experimental conclusions that can be drawn.

Figure 4a shows that without ECDM, the abrasive tool is easily clogged by the soft matrix metal and the problem of tool

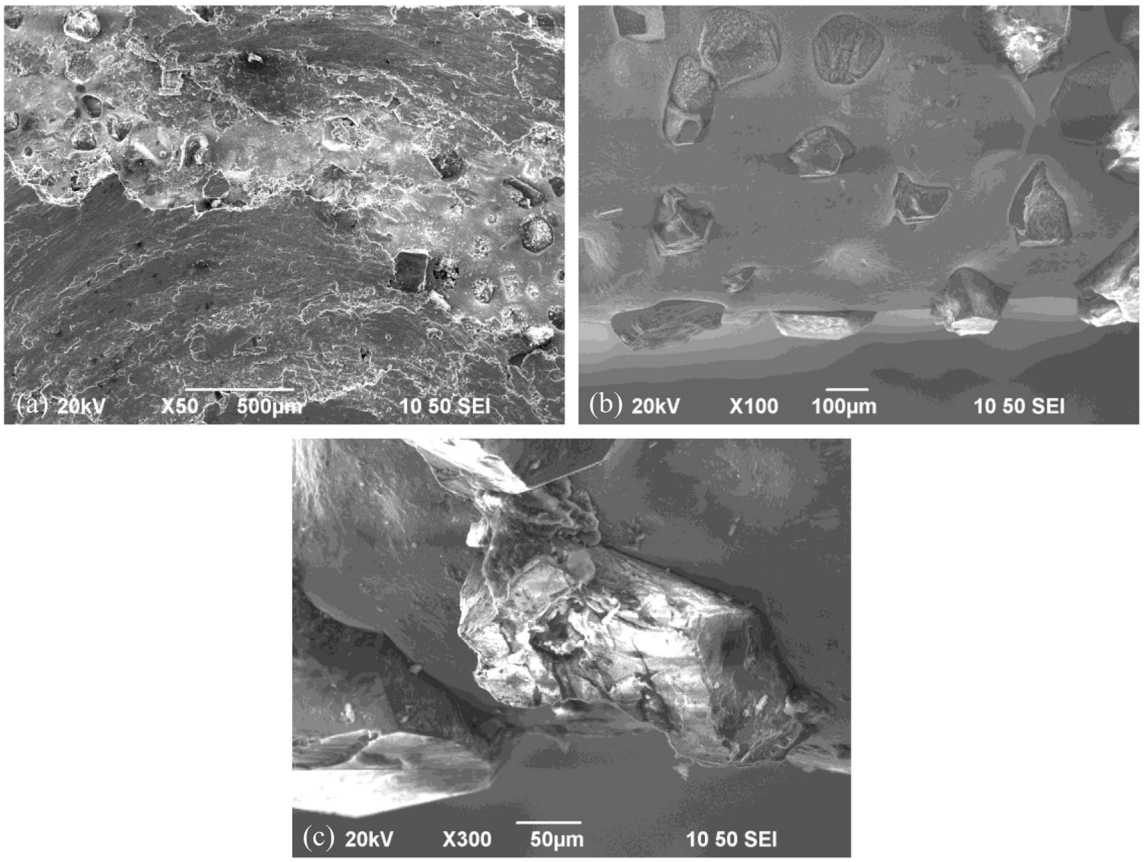

Fig. 4 SEM photographs showing the tool surfaces after machining the MMC under **a** processing condition A, **b** processing condition B, and **c** processing condition C

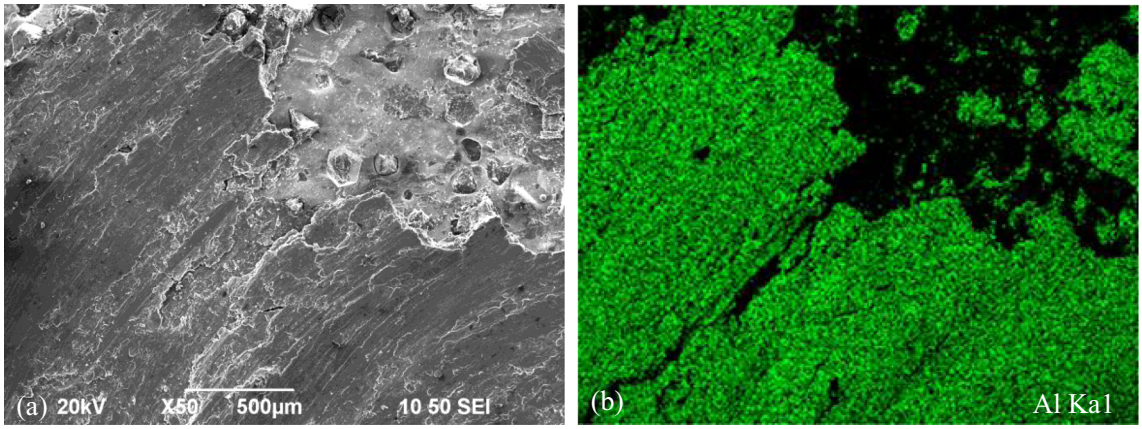

Fig. 5 EDS mapping of Al of the direct grinding tool surface. **a** An image of the tool surface after 1 min of grinding. **b** Mapping of Al

clogging is severe, even only after 1 min of grinding time, all the grits are covered by machining debris. However, tool clogging was hardly observed on the tool after 30 min G-ECDM of the MMC (Fig. 4b). An SEM-EDS mapping of aluminum element on the surfaces of the direct grinding tool (Fig. 5) and the G-ECDM tool (Fig. 6) confirms that the chips are Al-based and therefore belong to the workpieces. This clearly demonstrates the tool cleaning effect from EDM sparks.

In the presence of ECDM, even after G-ECDM for 60 min, only a small amount of debris can be found on the tool (Fig. 4c). Moreover, there is no sign of serious damage at the interface between the diamond grits and the binding material.

However, occasionally, microcracks can be observed on the G-ECDM tool surface (Fig. 7) (the processing conditions are given in Table 2, condition D). This is likely to be due to EDM sparking occurring near/at the chip-diamond grit

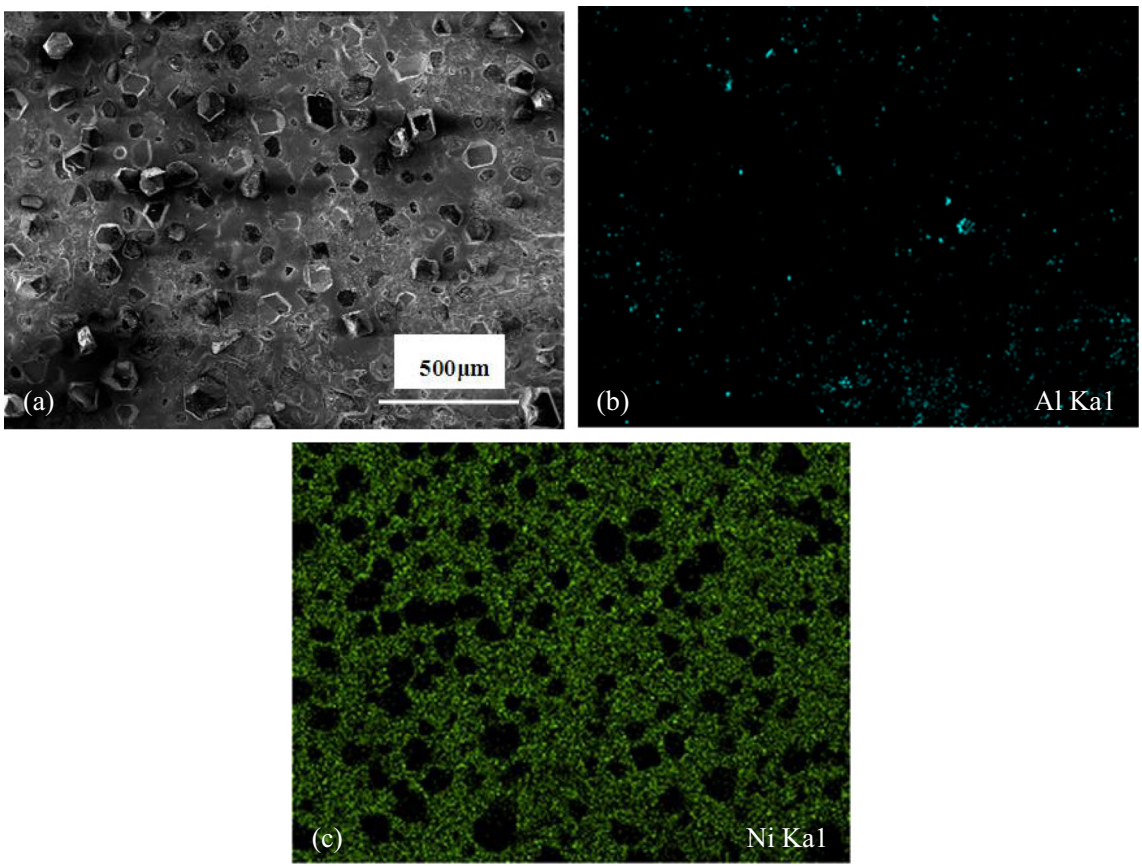

Fig. 6 EDS mapping of Al and Ni of the G-ECDM tool surface. **a** An image of the tool surface after 30 min of machining. **b** Mapping of Al on the tool. **c** Mapping of Ni on the tool

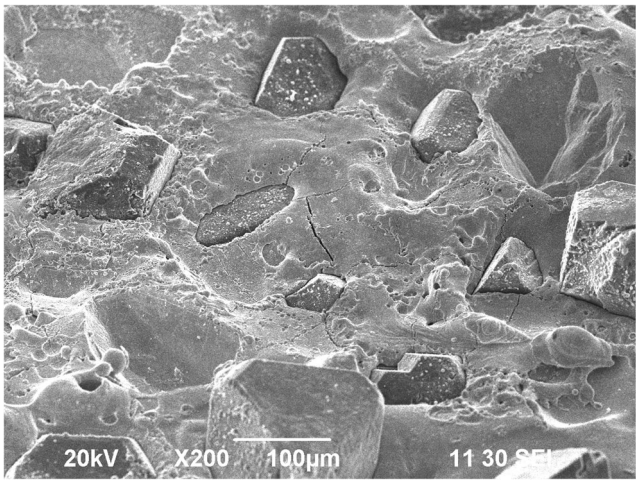

Fig. 7 SEM photography of the G-ECDM tool surface where microcracks are found (processing condition D)

interface. Therefore, if the amount and the volume of the clogged material are small and the arc energy is large, high thermal stresses could develop and result in thermal cracking. To avoid such a problem, further study is required to establish the condition where, on one hand there are enough chips to protect the tool electrode from excessive thermal stresses, while on the other hand a stable machining condition is maintained.

To further give support to the theory that machining chips can provide protection to the tool electrode in G-ECDM, a series of ECDM experiments were conducted (Table 2 processing conditions E and F).

Figures 8, 9, and 10 show the tool surface originally, and after a machining time of 3 and 5 min, respectively. It was found that for the case of 3 min processing time, with the removal of the Ni, many abrasive grits fell off from the tool surface (Fig. 9); while for the case of 5 min processing time, it is clear that more Ni has been removed and almost all of the abrasive grits were detached (Fig. 10). This clearly shows that EDM sparks could seriously damage the tool and remove the Ni binding material at this stage.

To study the relative strength and proportion of the ECM effect and EDM effect in the G-ECDM process, single-pulse experiments have been conducted by employing deionized water and electrolyte as the working medium respectively (Table 2 conditions G and H). Obviously, only the EDM effect exists in deionized water medium, while both an EDM and

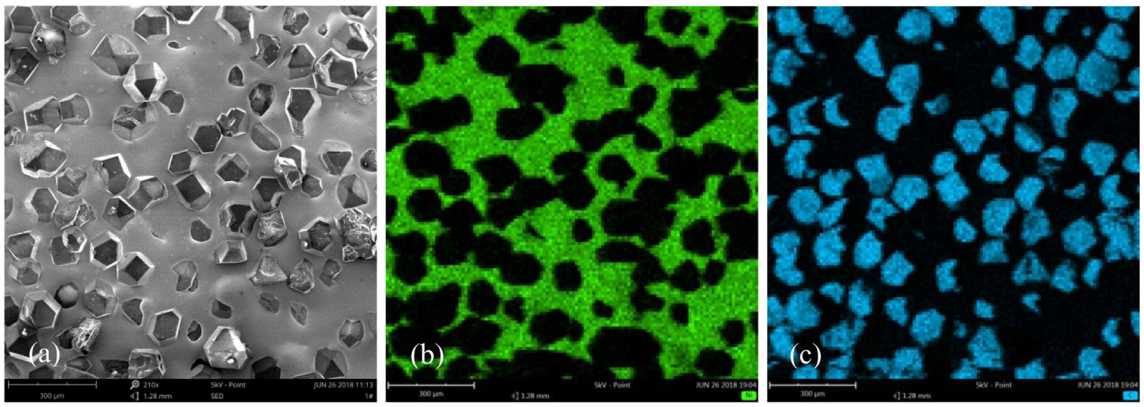

Fig. 8 EDS mapping of Ni and abrasive grits on an original tool surface. **a** Image of tool surface. **b** Ni mapping. **c** Grits mapping

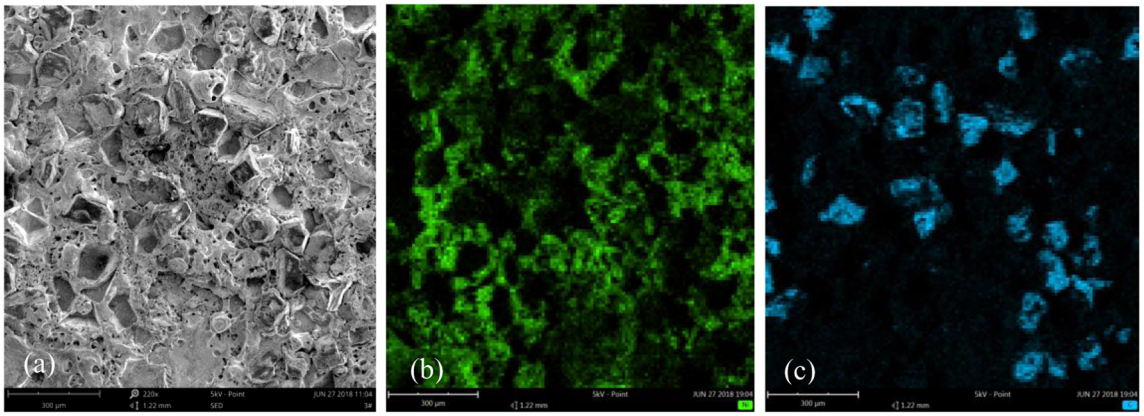

Fig. 9 EDS mapping of Ni and abrasive grits of the tool surface after 3 min machining (processing condition E). **a** Image of the machined surface. **b** Ni mapping. **c** Grits mapping

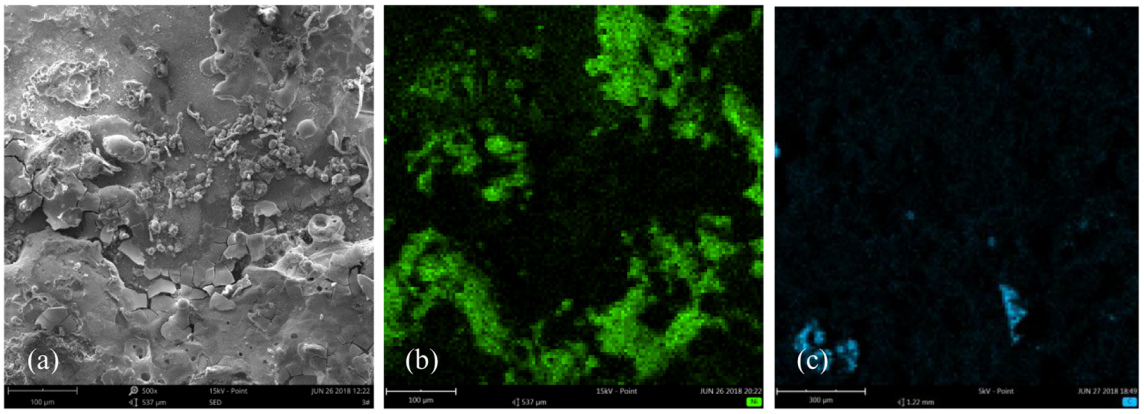

Fig. 10 EDS mapping of Ni and abrasive grits of the tool surface after 5 min machining (processing condition F). **a** Image of the machined surface. **b** Ni mapping. **c** Grits mapping

ECM effect exist in the electrolyte medium. The single-pulse crater volume in both media was measured using a 3-D optical device (Alicona IFM G4). Five measurements were taken to get an average for both processes, and the relative standard deviation (RSD) of the measurements is within 2%. It was found that the crater in electrolyte medium is approximately 31×10^5 μm^3 which is about 20% smaller than the one obtained in deionized water medium (39×10^5 μm^3) (Figs. 11 and 12). This is mainly due to the fact that during the process, the pulse energy is roughly divided into two parts, the ECM energy and the EDM spark energy. And under these experimental conditions, though the mechanism for the energy distribution is still not completely certain, almost 20% of total pulse energy is used to produce the ECM effect.

Compared to such rapid tool wear in the case of ECDM, G-ECDM exhibits a different property. For the case of G-ECDM, it

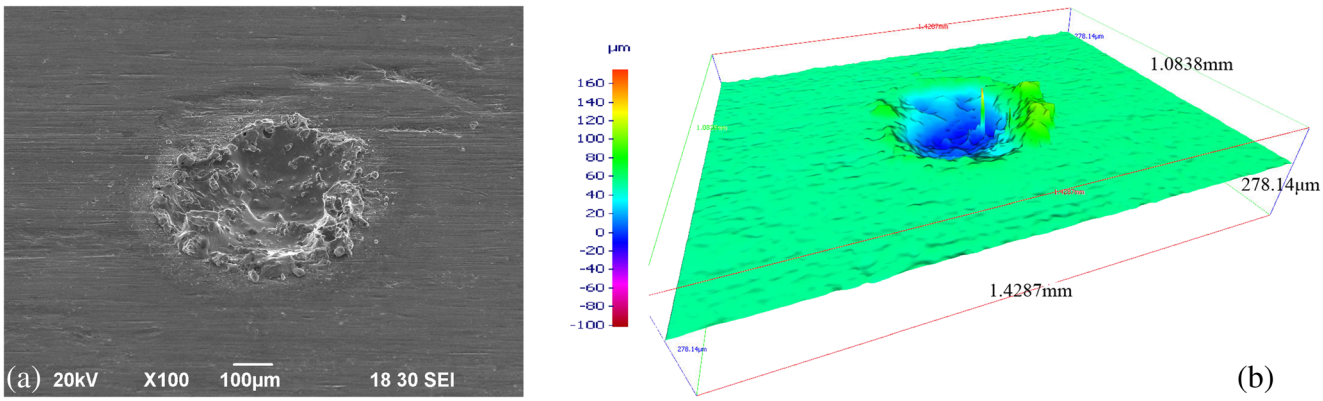

Fig. 11 Single-pulse crater produced in deionized water. **a** SEM photography. **b** Morphology of the crater

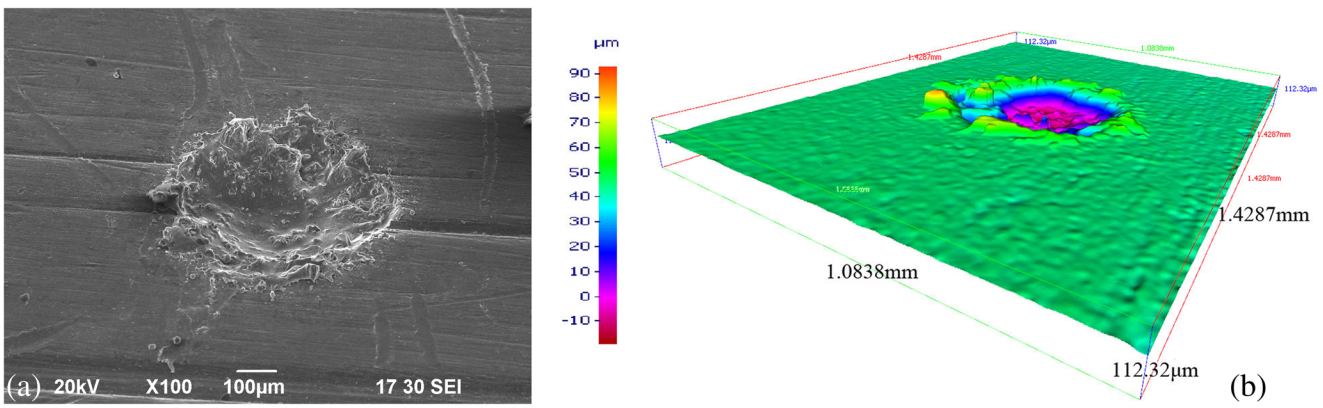

Fig. 12 Single-pulse crater produced in electrolyte. **a** SEM photography. **b** Morphology of the crater

was found that even, after a machining time of 30 min, the Ni layer still remains on the tool (Fig. 6). So, once again, this demonstrates that the Ni layer on the G-ECDM tool surface has been protected by the clogged material between the diamond grits. This means that the tool life of the G-ECDM tool would be governed by tool wear of the diamond grit and not so much by the ECDM action on the metal phase of the tool. It is therefore believed that good tool life is expected of the G-ECDM process.

3.2 A study of the grit volume fractions and the average grit height of the G-ECDM tool electrode

Figure 13a–c shows the re-constructed surface topologies of the original tool surface, the tool after G-ECDM for 30 min (processing condition B), and G-ECDM for 60 min (processing condition C), respectively. The average

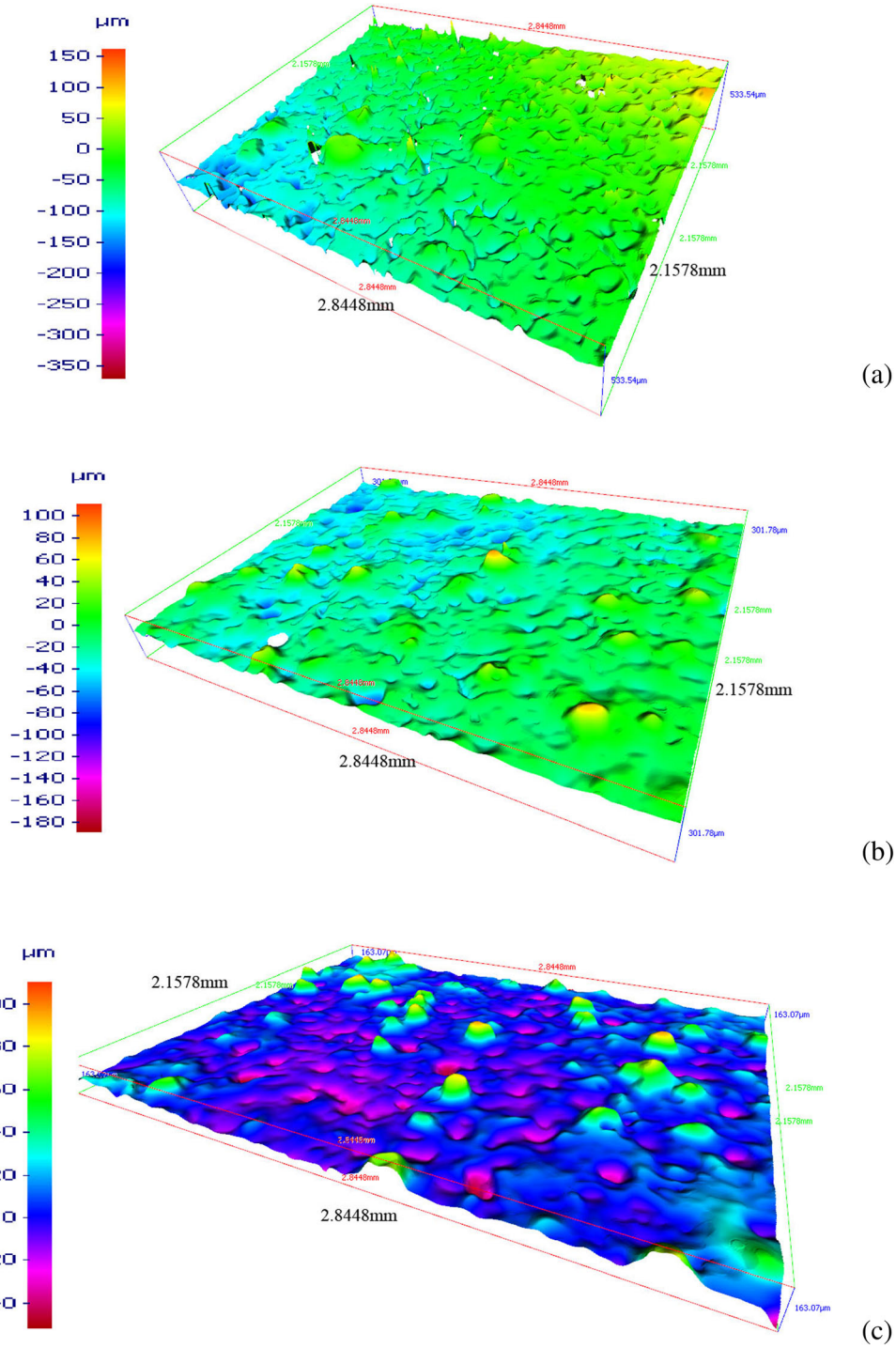

Fig. 13 Re-constructed surface topologies of **a** original tool, **b** tool after machining the MMC under processing conditions B, and **c** tool after machining under processing conditions C

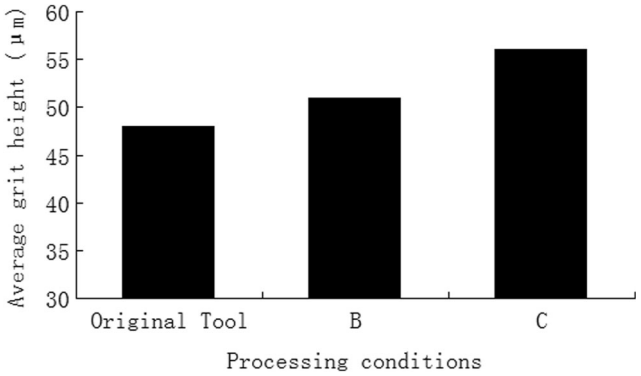

Fig. 14 Average grit height measured of the tool for the various processing conditions

diamond grit heights measured for these three conditions were 48 μm, 51 μm, and 56 μm, respectively (Fig. 14). The results show that the longer the processing time, the higher the grit height. It is believed that during G-ECDM, though the binding Ni layer of the tool is protected by the clogged material between the diamond grits, some material would still be removed by the ECDM action. The diamond grit volume fractions for three conditions were measured to be 0.55, 0.48, and 0.46 respectively (Fig. 15). Although there was a relatively large decrease in grit volume after 30 min into the machining, further machining only caused a very mild reduction. The relatively high detachment rate of diamond grit at the early stage of the machining is believed to be due to the fact that some grits were not well bonded to the Ni binding layer, and as a result, those loose grits detached from the tool. After the run-in period, the grit volume fraction hardly changed. This also leads to the conclusion that though some Ni binding material on the tool surface was removed by the ECDM action, most of the diamond grits remained firmly bonded by the Ni matrix. This means that the tool life of the G-ECDM tool is primarily governed by the tool wear of the diamond grits itself.

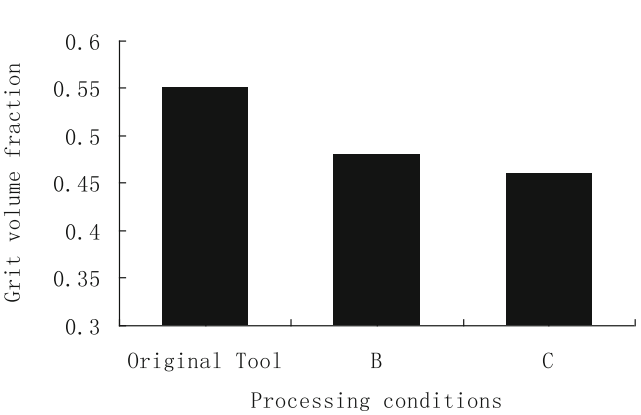

Fig. 15 Grit volume fraction remaining on the tool for the various processing conditions

4 Conclusions

(i) In G-ECDM, though the grinding action could cause tool clogging, the clogged material could be removed by the action of electrical discharging; thus, a stable processing condition might be maintained. On the other hand, the clogged material also provides protection to the tool; thus, long tool life is expected of the G-ECDM process. Therefore, a good balance between tool cleaning and tool protection must be reached so that the G-ECDM process can be operated effectively.

(ii) Although there was a relatively high detachment rate of the diamond grits at the early stage of the machining, the grit volume of the tool appeared to become rather stable after the run-in period. This means that the tool life of the G-ECDM tool is primarily governed by the tool wear of the diamond grit itself.

Funding information This research was supported by the National Natural Science Foundation of China (51675105), the Special Support Plan of the Guangdong province (2014TQ01X542), the Natural Science Foundation of Guangdong province (2017A0330313330), the Equipment pre-research foundation (61409230304), and the Fundamental Research Funds for the Central Universities (2015ZZ080).

References

1. Sharma P, Khanduja D, Sharma S (2014) Tribological and mechanical behavior of particulate aluminum matrix composites. J Reinf Plast Compos 33(23):2192–2202
2. Marsh G (2003) Next step for automotive materials. Mater Today 6(4):36–43
3. Akbari MK, Baharvandi HR, Shirvanimoghaddam K (2015) Tensile and fracture behavior of nano/micro TiB2 particle reinforced casting A356 aluminum alloy composites. Mater Des 66: 150–161
4. Shirvanimoghaddam K, Khayyam H, Abdizadeh H, Akbari MK, Pakseresht AH, Abdi F, Abbasi A, Naebe M (2016) Effect of B 4 C, TiB2 and ZrSiO4 ceramic particles on mechanical properties of aluminium matrix composites: experimental investigation and predictive modelling. Ceram Int 42(5):6206–6220
5. Nicholls CJ, Boswell B, Davies IJ, Islam MN (2017) Review of machining metal matrix composites. Int J Adv Manuf Technol 90(9–12):2429–2441
6. Zhao W, Huang S-J, Wu Y-J, Kang C-W (2017) Particle size and particle percentage effect of AZ61/SiCp magnesium matrix micro- and nano-composites on their mechanical properties due to extrusion and subsequent annealing. Metals 7(8):293
7. Si C, Tang X, Zhang X, Wang J, Wu W (2017) Microstructure and mechanical properties of particle reinforced metal matrix composites prepared by gas-solid two-phase atomization and deposition technology. Mater Lett 201:78–81
8. Ciftci I, Turker M, Seker U (2004) CBN cutting tool wear during machining of particulate reinforced MMCs. Wear 257(9):1041–1046

9. Aramesh M, Attia HM, Kishawy HA, Balazinski M (2017) Observation of a unique wear morphology of cBN inserts during machining of titanium metal matrix composites (Ti-MMCs); leading to new insights into their machinability. Int J Adv Manuf Technol 92(1–4):519–530
10. Ilio AD, Paoletti A (2000) A comparison between conventional abrasives and superabrasives in grinding of SiC-aluminium composites. Int J Mach Tool Manu 40(2):173–184
11. Yue TM, Lau WS (1996) Pulsed Nd:YAG laser cutting of Al/Li/SiC metal matrix composites. Adv Manuf Process 11(1):17–29
12. Zhong Z, Hung NP (2000) Diamond turning and grinding of aluminum-based metal matrix composites. Adv Manuf Process 15(6):853–865
13. Ahamed AR, Asokan P, Aravindan S, Prakash MK (2010) Drilling of hybrid Al-5%SiC-5%BC metal matrix composites. Int J Adv Manuf Technol 49(9–12):871–877
14. Li X, Bai F, Fu Y (2017) The small hole helical mill-grinding process and application in high volume fraction SiCp/Al MMCs. Int J Adv Manuf Technol 91(9–12):3007–3014
15. Xiong Y, Wang W, Jiang R, Lin K, Song G (2016) Tool wear mechanisms for milling in situ TiB2 particle-reinforced Al matrix composites. Int J Adv Manuf Technol 86(9–12):1–10
16. Kong X, Zhang H, Yang L, Chi G, Wang Y (2016) Carbide tool wear mechanisms in laser-assisted machining of metal matrix composites. Int J Adv Manuf Technol 85(1–4):365–379
17. Kök M, Kanca E, Eyercioğlu Ö (2011) Prediction of surface roughness in abrasive waterjet machining of particle reinforced MMCs using genetic expression programming. Int J Adv Manuf Technol 55(9–12):955–968
18. Hreha P, Radvanská A, Hloch S, Peržel V, Królczyk G, Monková K (2015) Determination of vibration frequency depending on abrasive mass flow rate during abrasive water jet cutting. Int J Adv Manuf Technol 77(1–4):763–774
19. Mohan B, Rajadurai A, Satyanarayana KG (2004) Electric discharge machining of Al–SiC metal matrix composites using rotary tube electrode. J Mater Process Technol 153–154(1):978–985
20. Ahamed AR, Asokan P, Aravindan S (2009) EDM of hybrid Al–SiC p –B 4 C p and Al–SiC p –glass p MMCs. Int J Adv Manuf Technol 44(5–6):520–528
21. Hourmand M, Farahany S, Sarhan AAD, Noordin MY (2015) Investigating the electrical discharge machining (EDM) parameter effects on Al-Mg 2 Si metal matrix composite (MMC) for high material removal rate (MRR) and less EWR–RSM approach. Int J Adv Manuf Technol 77(5–8):831–838
22. Garg RK, Singh KK, Sachdeva A, Sharma VS, Ojha K, Singh S (2010) Review of research work in sinking EDM and WEDM on metal matrix composite materials. Int J Adv Manuf Technol 50(5–8):611–624
23. Yan BH, Tsai HC, Huang FY, Long CL (2005) Examination of wire electrical discharge machining of Al 2 O 3 p/6061Al composites. Int J Mach Tool Manu 45(3):251–259
24. Rao TB, Krishna AG (2014) Selection of optimal process parameters in WEDM while machining Al7075/SiCp metal matrix composites. Int J Adv Manuf Technol 73(1–4):299–314
25. Rao SR (2012) Effect of process variables on metal removal rate in electrochemical machining of Al-B4C composites. Arch Appl Sci Res
26. Rao SR, Padmanabhan G, Naidu KM, Reddy AR (2014) Parametric study for radial over cut in electrochemical drilling of Al-5%B 4 C p composites ☆. Procedia Eng 97:1004–1011
27. Liu JW, Chen GX, Yue TM, Guo ZN (2012) Single pulse study of electrochemical discharge machining of metal matrix composites. Appl Mech Mater 200:536–539
28. Praneetpongrung C, Fukuzawa Y, Nagasawa S, Yamashita K (2010) Effects of the EDM combined ultrasonic vibration on the machining properties of Si3N4. Mater Trans 51(11):2113–2120
29. Sidhu SS, Batish A, Kumar S (2014) Study of surface properties in particulate-reinforced metal matrix composites (MMCs) using powder-mixed electrical discharge machining (EDM). Adv Manuf Process 29(1):46–52
30. Kumar H (2015) Development of mirror like surface characteristics using nano powder mixed electric discharge machining (NPMEDM). Int J Adv Manuf Technol 76(1–4):105–113
31. Pramanik A, Basak AK, Islam MN (2015) Effect of reinforced particle size on wire EDM of MMCs. Int J Mach Mach Mater 17(2):139
32. Hocheng H, Lei WT, Hsu HS (1997) Preliminary study of material removal in electrical-discharge machining of SiC/Al. J Mater Process Technol 63(1–3):813–818
33. Mahdavinejad RA, Mahdavinejad A (2005) ED machining of WC–Co. J Mater Process Technol 162(10):637–643
34. Lohrengel MM, Rataj KP, Münninghoff T (2016) Electrochemical machining—mechanisms of anodic dissolution. Electrochim Acta 201:348–353
35. Liu JW, Yue TM, Guo ZN (2010) An analysis of the discharge mechanism in electrochemical discharge machining of particulate reinforced metal matrix composites. Int J Mach Tool Manu 50(1):86–96
36. Liu JW, Yue TM, Guo ZN (2013) Grinding-aided electrochemical discharge machining of particulate reinforced metal matrix composites. Int J Adv Manuf Technol 68(9–12):2349–2357